Archives of Biochemistry and Biophysics 532 (2013) 46–53

Contents lists available at SciVerse ScienceDirect

Archives of Biochemistry and Biophysics

journal homepage: www.elsevier.com/locate/yabbi

Tryptophan-47 in the active site of *Methylophaga sp.* strain SK1 flavin-monooxygenase is important for hydride transfer

Andre Han [a], Reeder M. Robinson [a], Somayesadat Badieyan [a], Jacob Ellerbrock [a], Pablo Sobrado [a,b,c,*]

[a] Department of Biochemistry, Virginia Tech, Blacksburg, VA 24061, USA
[b] Virginia Tech Center for Drug Discovery, Virginia Tech, Blacksburg, VA 24061, USA
[c] Fralin Life Science Institute, Virginia Tech, Blacksburg, VA 24061, USA

ARTICLE INFO

Article history:
Received 31 October 2012
and in revised form 31 December 2012
Available online 25 January 2013

Keywords:
Flavin monooxygenases
Active site residue
Flavin
Hydride transfer
Kinetic isotope effects

ABSTRACT

Flavin-dependent monooxygenase (FMO) from *Methylophaga sp.* strain SK1 catalyzes the NADPH- and oxygen-dependent hydroxylation of a number of xenobiotics. Reduction of the flavin cofactor by NADPH is required for activation of molecular oxygen. The role of a conserved tryptophan at position 47 was probed by site-directed mutagenesis. FMOW47A resulted in an insoluble inactive protein; in contrast, FMOW47F was soluble and active. The spectrum of the flavin in the mutant enzyme was redshifted, indicating a change in the flavin environment. The k_{cat} values for NADPH, trimethylamine, and methimazole, decreased 5-8-fold. Primary kinetic isotope effect values were higher, indicating that hydride transfer is more rate-limiting in the mutant enzyme. This is supported by a decrease in the rate constant for flavin reduction and in the solvent kinetic isotope effect values. Results from molecular dynamics simulations show reduced flexibility in active site residues and, in particular, the nicotinamide moiety of $NADP^+$ in FMOW47F. This was supported by thermal denaturation experiments. Together, the data suggests that W47 plays a role in maintaining the overall protein flexibility that is required for conformational changes important in hydride transfer.

Published by Elsevier Inc.

Flavin-dependent monooxygenase from *Methylophaga sp.* strain SK1 (FMO) catalyzes the NADPH- and oxygen-dependent hydroxylation of several xenobiotics (Scheme 1) [1]. The reaction mechanism can be divided into oxidative and reductive half-reactions. In the reductive half-reaction, FMO reacts with NADPH leading to the formation of reduced flavin and $NADP^+$ (Scheme 1a and b). In the oxidative half-reaction, the reduced flavin reacts with molecular oxygen to form the C4a-hydroperoxyflavin, which is the hydroxylating species (Scheme 1c) [1,2]. In the presence of a substrate containing a soft-nucleophilic heteroatom, the enzyme is capable of transferring a single oxygen atom to the nucleophilic site, thereby oxygenating the substrate (Scheme 1d) [3].

Site-directed mutagenesis and structural studies have shown that the C4a-hydroperoxyflavin is stabilized by $NADP^+$, which remains bound throughout the catalytic cycle [4–7]. If this intermediate is not stabilized it decays to hydrogen peroxide and oxidized flavin. Thus, stabilization of this intermediate is essential for preventing uncoupling of the reaction. It has been shown that interactions of several residues with $NADP^+$ are important for placing the coenzyme in a position optimal for intermediate stabilization [7]. The active site of FMO contains a conserved tryptophan residue that is in a site opposite of the NADP(H) and xenobiotic binding sites [6]. This residue is conserved in all known FMO sequences and in other related Class B flavin-monooxygenases (Fig. 1). The work presented here describes the biochemical characterization and analysis of the effect of mutating W47 to probe the role of this residue in catalysis.

Materials and methods

Materials

Methimazole, glutathione, and trimethylamine hydrochloride were obtained from Sigma–Aldrich. pVP55A was obtained from the Center for Eukaryotic Structural Genomics, University of Wisconsin, Madison [8]. *Escherichia coli* BL21-TI^R cells were from Invitrogen. AccuPrime *Pfx* DNA Polymerase was from Invitrogen (Carlsbad, CA). The oligonucleotide primers used in the mutagenesis reactions were obtained from Integrated DNA Technology. Nucleotide sequencing was performed at the Virginia Bioinformatics Institute DNA Sequencing facility.

* Corresponding author at: Department of Biochemistry, Virginia Tech, Blacksburg, VA 24061, USA. Fax: +1 540 231 9070.
E-mail address: psobrado@vt.edu (P. Sobrado).

0003-9861/$ - see front matter Published by Elsevier Inc.
http://dx.doi.org/10.1016/j.abb.2013.01.004

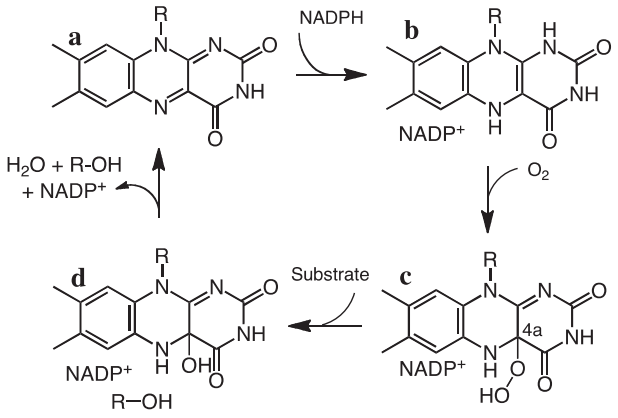

Scheme 1. Reaction catalyzed by FMO. The oxidized flavin (a) reacts with NADPH to form the reduced flavin and oxidized $NADP^+$ complex (b). The reduced enzyme is then able to react with molecular oxygen to form the C4a-hydroperoxyflavin intermediate (c). The stability of this intermediate depends on the presence of $NADP^+$ in the active site. After substrate binding, hydroxylation occurs and the hydroxylated flavin is formed (d). After flavin dehydration, release of $NADP^+$ and hydroxylated product, the oxidized flavin is formed for the next catalytic cycle.

Cloning and mutagenesis

The gene encoding for FMO was synthesized and codon optimized for expression in *E. coli* (GenScript, NJ). The nucleotide sequence recognized by the enzymes *Sgf*I and *Pme*I were added at the 5′ and 3′ ends, respectively. The gene, digested with *Pme*I and *Sgf*I restriction endonucleases, was ligated into the pVP55A plasmid, which was previously digested with the same enzymes. Mutation of W47 in FMO to F or A was performed using the QuikChange method (Agilent Technologies, Santa Clara, CA). Primers used are shown in Table 1S.

Protein expression and purification

The gene coding for FMO was cloned into the pVP55A plasmid such that the recombinant protein was expressed as an *N*-terminal 8xHis fusion. A single colony of BL21-TI^R cells transformed with pVP55Afmo was used to inoculate 50 mL Luria–Bertani (LB) medium (100 μg/mL ampicillin), and incubated at 37 °C. The next day, six fernbach flasks containing 1.5 L LB medium (100 μg/mL ampicillin) were each inoculated with 10 mL of the overnight culture. After reaching an optical density value of ~0.6 at 600 nm (OD_{600}), isopropyl β-D-1-thiogalactopyranoside was added at 100 μM final concentration and the temperature lowered to 15 °C overnight. The cells were harvested via centrifugation at 8,000*g* and the resulting pellet (~40 g) was stored at −80 °C. For purification, the cell pellet was thawed and resuspended in 150 mL of buffer A (25 mM HEPES, 125 mM NaCl, 5 mM imidazole) and 25 μg/mL of DNase, RNase, and lysozyme were added. The solution was stirred for 40 min at 4 °C. Cells were then lysed by sonication for

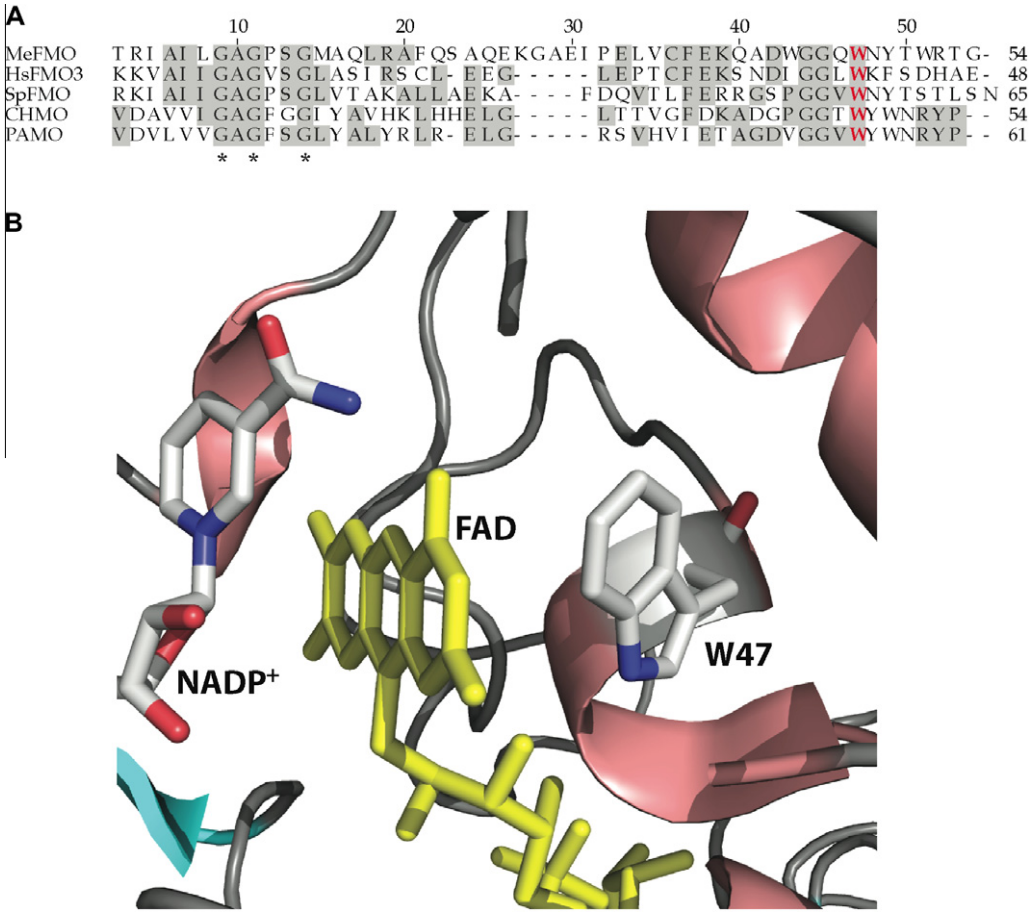

Fig. 1. (A) Amino acid sequence alignment of members of the Class B flavin-dependent monooxygenases (MeFMO, flavin monooxygenase from *Methylophaga sp.* strain SK1; HsFMO3, *Homo sapiens* flavin monooxygenase isoform 3; SpFMO, *Schizosacchromyces pombe* flavin monooxygenase; CHMO, cyclohexanone monooxygenase; PAMO, phenylacetone monooxygenase). The flavin binding motif (GXGXXG) is shown with asterisks. The conserved tryptophan corresponding to W47 in FMO is shown in red. The alignment was performed using Clustal W. (B) Position of W47 in the active site of *Methylophaga sp.* strain SK1 FMO. The figure was made using Pymol (PDB code 2vq7). (For interpretation of the references to color in this figure legend, the reader is referred to the web version of this article.)

Table 1
Steady-state kinetic parameters wild-type and W47F FMO.

Substrate	Wild-type			W47F		
	k_{cat} (s^{-1})	K_m (μM)	k_{cat}/K_m (μM^{-1} s^{-1})	k_{cat} (s^{-1})	K_m (μM)	k_{cat}/K_m ($\mu M^{-1}s^{-1}$)
Trimethylamine	6.1 ± 0.1	2.6 ± 0.3	2.3 ± 0.3	1.25 ± 0.05	1.5 ± 0.3	0.8 ± 0.2
Methimazole	2.7 ± 0.1	163 ± 15	0.016 ± 0.002	0.67 ± 0.05	37 ± 8	0.018 ± 0.004
NADPH	7.3 ± 0.1	4.1 ± 0.4	1.8 ± 0.2	0.92 ± 0.01	4.3 ± 0.3	0.21 ± 0.02
NADPH[a]	0.080 ± 0.006	n.d.	n.d.	0.17 ± 0.01	n.d.	n.d.
Oxygen[b]	7.7 ± 0.3	19 ± 3	0.41 ± 0.07	2.7 ± 0.2	42 ± 9	0.06 ± 0.01

Conditions: 1 mL 25 mM Tris–HCl, 35 mM NaCl, 30 mM EDTA, pH 8.5 at 25 °C.
n.d. – not determined.
[a] Oxidase activity (in the absence of second substrate).
[b] At saturating concentrations of trimethylamine and NADPH.

10 min (10 s on, 20 s off) at 60% amplitude on ice and centrifuged at 40,000*g* for 40 min. The resulting supernatant was loaded onto three in-tandem 5 mL nickel immobilized metal affinity chromatography (IMAC) HisTrap columns (GE Healthcare) that were previously equilibrated with buffer A. The column was then washed with buffer A and the bound protein eluted with 25 mM HEPES, 125 mM NaCl, and 300 mM Imidazole. The fractions containing the 8×His-FMO protein were collected and concentrated using an Amicon stirred cell pressure concentrator and diluted with buffer A. The sample was concentrated again using the same method. The concentrated sample was then injected into a HiPrep 26/10 Desalting Column (GE Healthcare), which was equilibrated and eluted with 25 mM HEPES and 125 mM NaCl. The protein was concentrated and flash frozen into droplets using liquid nitrogen and stored at −80 °C. FMOW47F protein was subjected to the same purification protocol with addition of 5% glycerol in all buffer solutions.

Oxygen consumption assay

The activity of FMO was assayed by measuring the rate of oxygen consumption using a Hansatech Oxygraph system (Hansatech, Norfolk, UK). The activity was measured using methimazole and trimethylamine as the hydroxyable substrates and NADPH as the source of reducing equivalents. The assay was performed in 1 mL 25 mM Tris–HCl, 35 mM NaCl, and 30 mM Ethylenediaminetetraacetatic acid (EDTA), pH 8.5 at 25 °C. Prior to each assay, the buffer solution was shaken vigorously to maintain an air-saturated concentration of dissolved oxygen. The assay was initiated by addition of 0.5 or 1.2 μM of wild-type or W47F FMO, respectively. The decrease in oxygen concentration was measured over the course of 2 min. Trimethylamine was varied from 1 to 40 μM, and methimazole from 10 to 450 μM, while saturating with NADPH (100 μM). Glutathione (0.5 mM) was added in assays where methimazole was used as substrate [9]. In assays where the kinetic parameters for NADPH were determined, the concentration of trimethylamine was saturating (20 μM) and NADPH varied from 4 to 75 μM.

In order to determine the kinetic parameters as a function of oxygen concentration, trimethylamine and NADPH were present at saturating levels (100 μM). Various concentrations of oxygen (25 to 273 μM) were obtained by bubbling the assay solution with different gas mixtures of 100% oxygen and nitrogen. The initial rates were plotted as a function of the variable substrate and the data was fit to the Michaelis–Menten equation.

Oxidase activity

The oxidase activity was determined by measuring oxygen consumption at saturating concentrations of NADPH (100 μM) in the absence of the second substrate.

Kinetic isotope effects (KIEs)

pro-R-NADPD and NADPH were synthesized following published protocols [10,11]. The rate of oxygen consumption was determined as indicated above in 1 mL 25 mM Tris–HCl (pH 8.5) 35 mM NaCl, 30 mM EDTA, trimethylamine (20 μM) at varying NADPD or NADPH concentrations. The KIE on the rate of flavin reduction (k_{red}) was measured by monitoring the change in absorbance (442 nm, for wild-type FMO and 456 nm, for FMOW47F) on an Applied Photophysics SX20 stopped-flow spectrometer (Surrey, UK), under anaerobic conditions as previously described [11]. All solutions were made in anaerobic 100 mM sodium phosphate pH 7.5, at 15 °C. Freshly synthesized NADP(D/H) was used at 0.5 mM concentration after mixing. To obtain the rate of flavin reduction, the changes in absorbance were fit to Eq. (1). In this biphasic exponential equation, *a* and *k* are the amplitude and first-order rate constant, respectively, of the first (1) or second (2) phase, and C is the final absorbance. Solvent KIEs were determined by measuring the rate of oxygen consumption with 100 μM NADPH, 100 mM sodium phosphate, pH 7.5, in 99% deuterium oxide at varying trimethylamine concentrations (4–40 μM).

$$A_t = c + a_1 e^{-(k_1 * t)} + a_2 e^{-(k_2 * t)} \quad (1)$$

Molecular dynamics (MD) simulations

The crystal structure of wild type flavin-containing monooxygenase (wtFMO) (chain A) in complex with $NADP^+$ from *Methylophaga* sp. strain SK1 (PDB code: 2VQ7) [12] and its FMOW47F mutant (in silico mutation) were subjected to explicit MD simulations using Gromacs 4.5.5 with parameters from the united-atom Gromos96 53A6 force field [6]. The flavin adenine dinucleotide (FAD) topology was formed from the existing adenosine triphosphate (ATP) and flavin mononucleotide (FMN) topologies where force field and both FAD and $NADP^+$ were simulated in their oxidized state. Before the simulation, the pKa values for ionizable amino acid residues at a pH of 7.5 (optimum pH for this enzyme) were estimated using the H++ program [12], and hydrogen atoms were added based on these predictions. While keeping the original crystal waters, SPC water molecules [13,14], and Na^+/Cl^- ions, to approximate a final concentration of 100 mM, were added to neutralize the net charge of the system. The parameters for system preparation, energy minimization, equilibration, and MD production were set up as previously described [15]. All simulations were conducted at 300 K. Analyses were performed using utilities available in the GROMACS suite of programs or by scripts written in-house.

Differential scanning fluorimetry

The T_m of wtFMO and FMOW47F were determined using a Bio-Rad CFX96 Touch Real-Time PCR Detection System. Each reaction

was performed in a final volume of 30 μL, 100 mM sodium phosphate, pH 7.5. Each condition contained 5 μM enzyme, 5×SYPRO Orange, and 0 or 100 μM $NADP^+$. The SYPRO orange was excited at 492 nm and emission was detected at 610 nm after incubation for 30 s at 0.5 °C intervals from 10 °C to 80 °C. Each experiment was performed in triplicate.

Results and discussion

Protein expression and purification

FMOW47F was expressed and purified following procedures previously developed for the wild-type enzyme [6]. The purified enzyme was stable and contained tightly bound FAD. The flavin spectra of FMOW47F appeared to have been modified by the mutation. A clear shift of the peak at 442 nm in the wild-type enzyme to 456 nm in the W47F mutant was observed. This change in the flavin spectra indicates changes in the environment of the flavin active site. FMOW47A was also created and the enzymes expressed. However, the resulting protein was found in the insoluble fraction after sonication and centrifugation. Therefore, we only characterized the FMOW47F enzyme.

Steady-state kinetic parameters

The activity of both wild-type and W47F FMO were tested with trimethylamine and methimazole as substrates and NADPH as the coenzyme. The data is summarized in Table 1. A general decrease in the k_{cat} values of ~5-fold was observed when trimethylamine and methimazole were the variable substrates. The k_{cat}/K_m values

Table 2
Primary and solvent deuterium kinetic isotope effects.

Parameter	Wild-type	W47F
$^{D}k_{cat}$	3.1 ± 0.1	3.8 ± 0.2
$^{D}(k_{cat}/K_m)$	2.5 ± 0.2	3.3 ± 0.3
$^{D2O}k_{cat}$	2.1 ± 0.1	1.4 ± 0.1
$^{D2O}(k_{cat}/K_m)$	1.3 ± 0.3	1.1 ± 0.3
$^{D}k_{red}$	2.8 ± 0.1	4.3 ± 0.1

Conditions: 1 mL 25 mM Tris–HCl, 35 mM NaCl, 30 mM EDTA, pH 8.5 at 25 °C.

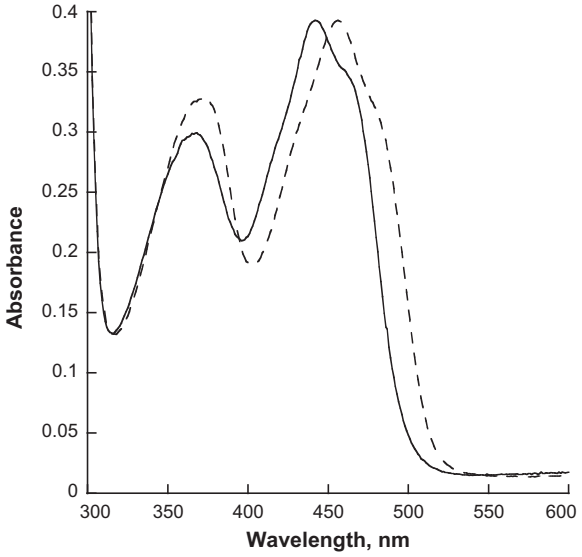

Fig. 2. Spectra of the flavin cofactor in wtFMO (solid lines) and FMOW47F (dashed lines). For the wild-type enzyme, the λ_{max} is at 442 nm while in the FMOW47F the λ_{max} is at 456 nm.

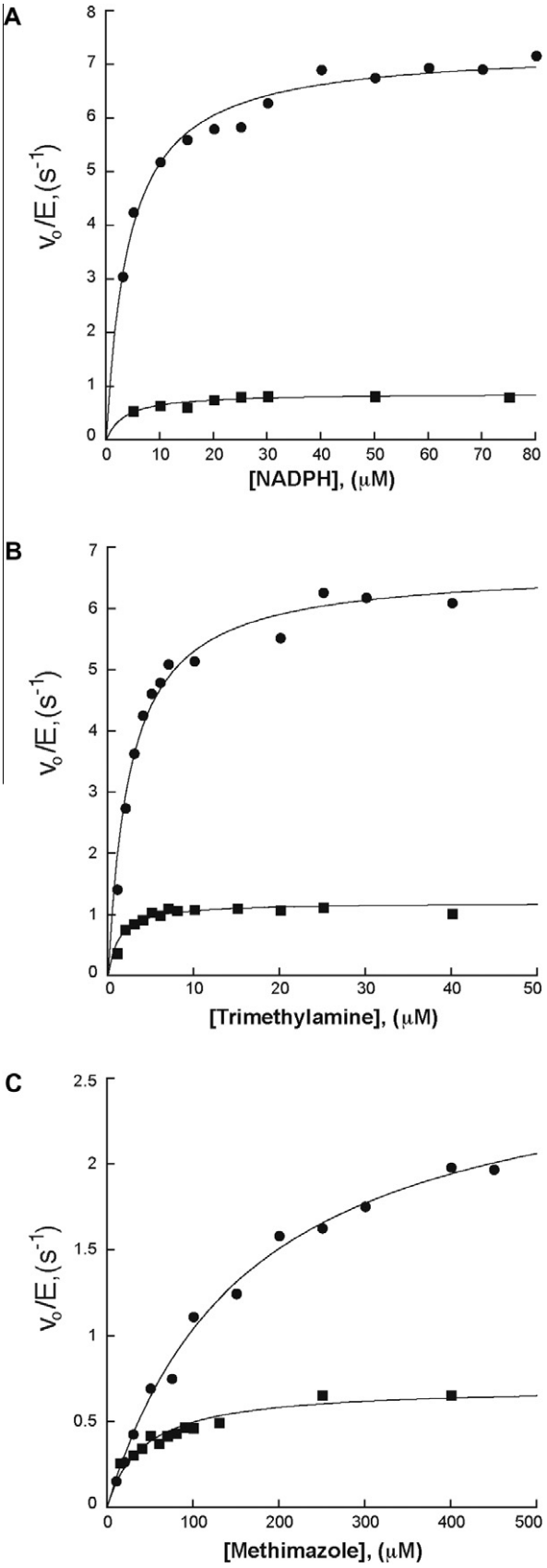

Fig. 3. Steady-state kinetics of wtFMO (circles) and FMOW47F (squares). The activity was determined by measuring the rate of oxygen consumption as a function of NADPH (A), trimethylamine (B), and methimazole (C).

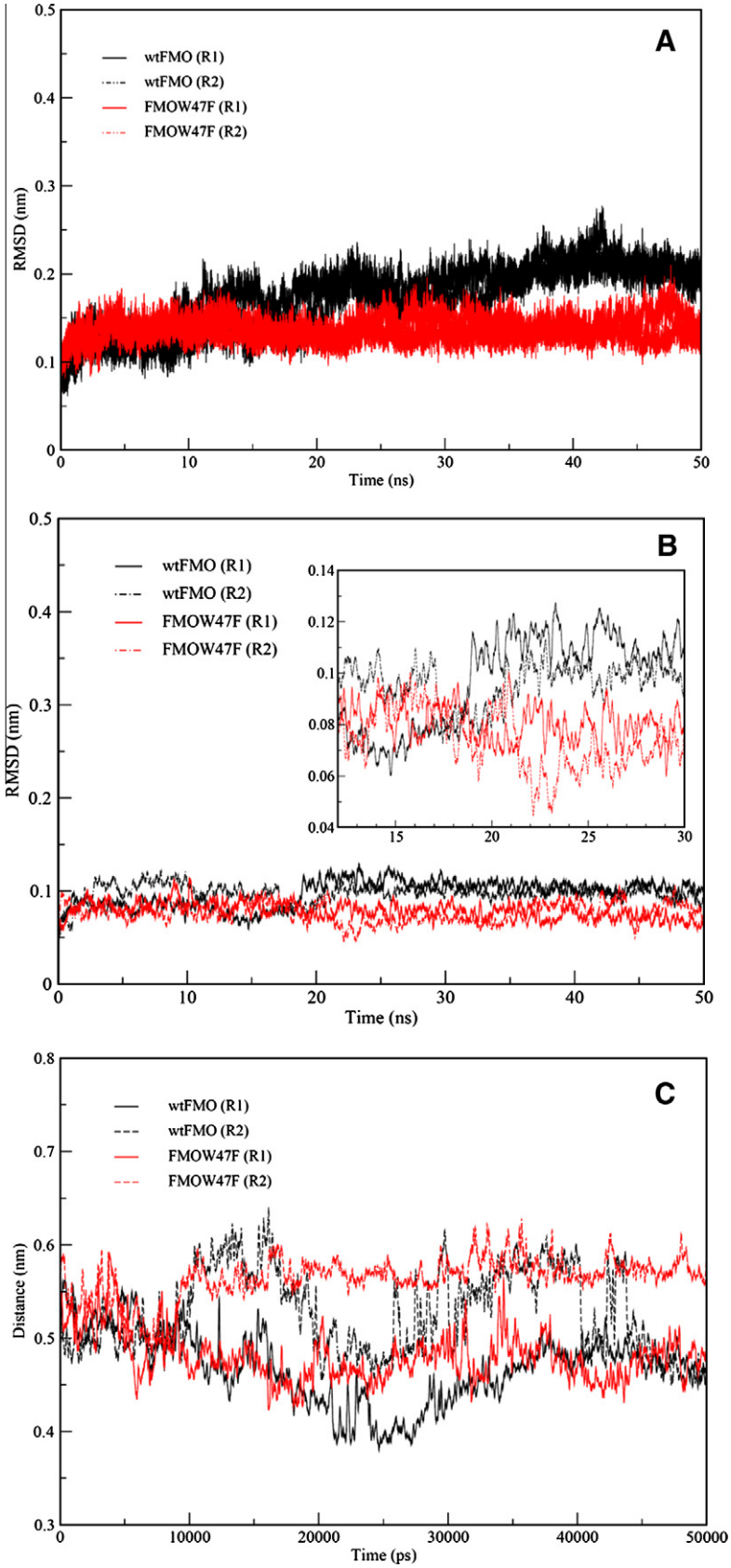

Fig. 4. 50 ns MD simulations of wtFMO and FMOW47F. RMSD of interacting residues (backbone) to isoalloxazine and nicotinamide moieties during simulation (A), RMSD of nicotinamide part of $NADP^+$ (B), N5 (FAD)–C4N ($NADP^+$) distance during simulation (C). R1 and R2 indicate the replicate of each simulation.

decreased only 3-fold for trimethylamine. When NADPH was the variable substrate and trimethylamine was kept constant, an ~8-fold decrease in both k_{cat} and k_{cat}/K_m values was measured. These results show that W47 plays a role in catalysis. To test if the mutation had an effect in the k_{cat} and k_{cat}/K_m values for oxygen, the activity was measured at saturating concentrations of NADPH and trimethylamine at various concentrations of oxygen (Fig. 1S). The kinetic parameters for oxygen in the mutant enzyme were only 2-fold different from the wild-type enzyme (Table 1).

Oxidase activity

We tested whether the presence of the tryptophan residue at position 47 was necessary for the stabilization of the C4a-hydroperoxyflavin intermediate. It has been shown that FMO is capable of reacting with NADPH to form a reduced FMO/$NADP^+$ complex (Scheme 1b). This complex can then react with molecular oxygen and form the C4a-hydroperoxyflavin intermediate, which is stabilized until the second substrate binds, otherwise it decays very slowly by releasing hydrogen peroxide [1]. The rate of oxygen consumption in the absence of trimethylamine or methimazole for FMOW47F was twice the value measured for the wild-type enzyme (Table 1) indicating that no major changes in the stabilization of the C4a-hydroperoxyflavin intermediate were caused by mutation of W47. This is consistent with recent biochemical and structural data indicating that the stabilization of this intermediate in FMO occurs via interaction with $NADP^+$ and other active site residues on the opposite side of the flavin [7].

Steady-state primary and solvent kinetic isotope effects

The solvent and primary deuterium KIE data are summarized in Table 2. Primary KIE were measured with NADP(H) as substrate to determined if W47 plays a role in the hydride transfer step. For

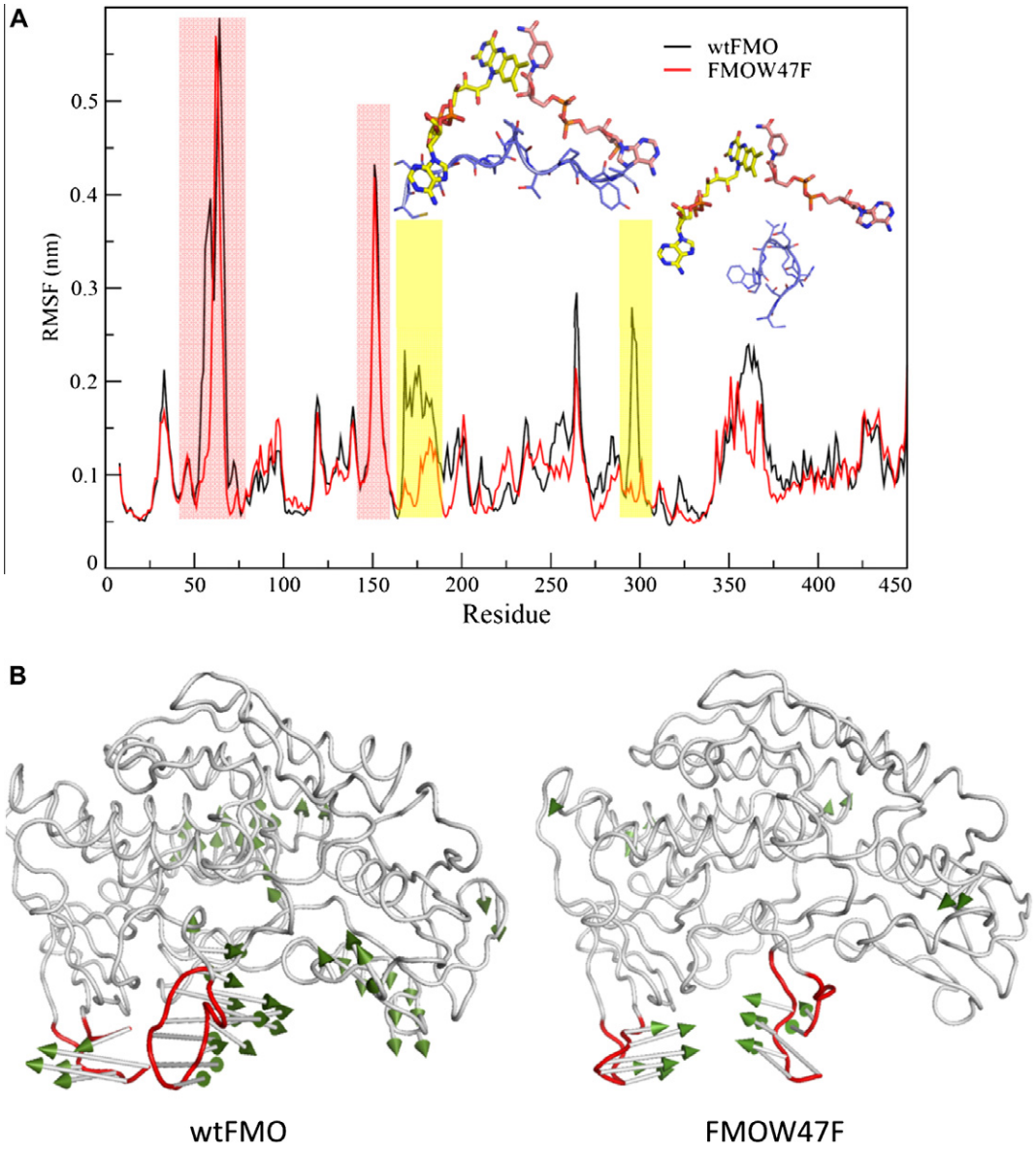

Fig. 5. RMSF plot of the protein backbone for wtFMO and FMOW47A (A). Each RMSF plot is averaged over the replicates for the last 30 ns of each simulation. Two regions of the protein backbone (highlighted in yellow) display fluctuations that are dependent on the W47F mutation, residues 165–175 and 293–300. The position of each loops relative to FAD and NADP are illustrated in figures nearby to that region on the plot. Two other regions, loop 56–68 and loop 149–155 (highlighted with pink bar), exhibit similar high fluctuation in both mutant and wild type enzyme. However, based on PCA analyses, movement direction of these two loops differ between the mutant and wild-type enzymes (B). (For interpretation of the references to color in this figure legend, the reader is referred to the web version of this article.)

wtFMO enzyme, $^{D}k_{cat}$ and $^{D}(k_{cat}/K_m)$ values of 3.1 and 2.5 were measured, respectively. These values indicate that hydride transfer is partially rate-limiting. Values for the mutant enzyme were higher. The $^{D}k_{cat}$ and $^{D}(k_{cat}/K_m)$ values were 3.8 and a 3.3, respectively, indicating that hydride transfer was more rate limiting in the mutant enzyme. A solvent KIE value of ~1 was measured for k_{cat}/K_m for wtFMO and FMOW47F. These results indicate that an exchangeable proton step is not in flight in the rate-limiting step before the first irreversible step. In contrast, a normal (>1) $^{D2O}k_{cat}$ value was determined for both enzymes. Thus, a protonation or deprotonation step is partially rate limiting for k_{cat}, perhaps flavin dehydration (Scheme 1a–d). For the FMOW47F enzyme, the solvent KIE are lower, consistent with the results that hydride transfer is more rate limiting in the mutant enzyme.

Rapid-reaction kinetics and primary kinetic isotope effects

The rate of flavin reduction, k_{red}, by NADPH was directly measured by monitoring the changes in flavin absorbance under anaerobic conditions. The k_{red} value for wild-type FMO was 24 ± 0.2 s^{-1}, consistent with previously published results [7]. For the FMOW47F enzyme, a k_{red} value of 8.5 ± 0.3 s^{-1} was determined (Fig. 2S). The decrease in the k_{red} value clearly indicates that replacement of W at position 47 negatively affects the hydride transfer step. This is further supported by the increase in the $^{D}k_{red}$ value for FMOW47F (Table 2) (Fig. 3).

MD simulations of wtFMO and FMOW47F

To assess the molecular impact of mutation on hydride transfer, we performed united atom MD simulations on both the wild-type and W47F mutant of FMO in complex to $NADP^+$. Analyses of root mean square deviation (RMSD) during a 50 ns simulation imply reduced flexibility in the active site residues (interacting with isoalloxazine and nicotinamide moieties) of FMOW47F compared to the wild-type enzyme (Fig. 4A). This difference is mainly seen in the mobility of the nicotinamide part of $NADP^+$ (Fig. 4B), which affects N5 (FAD) and C4 ($NADP^+$) distance. While in wild-type FMO, the N5-C4 distance appears to fluctuate during the simulation; in FMOW47F, the atoms establish an almost steady separation during simulations (Fig. 4C). Beside residues interacting with isoalloxazine and nicotinamide, analysis of root mean square fluctuation (RMSF) shows two other regions, loop 165–175 and loop 293–300, having reduced flexibility in FMOW47F (Fig. 5A, highlighted in yellow). Loop 165–175 is extended in a way that interacts with the adenosine moiety of both FAD and $NADP^+$. Loop 293–300 carries N296, which is in hydrogen bond distance from the phosphate group of $NADP^+$ and is highly rigid in the mutant enzyme (Fig. 5A).

The MD simulation data provided in this study may not perfectly reflect the complete impact of the W47F mutation on hydride transfer because there is no available structure for the oxidized enzyme in complex with NADPH. However, the rigidifying effect of the W47F mutation on the residues interacting with FAD and $NADP^+$ may be extended to the NADPH binding mode of FMO structure as well.

In addition, the Principal Component Analysis (PCA) of MD trajectories revealed two highly fluctuated loops (loop 56–68 and loop 149–155) moving toward each other in FMOW47F while they moved outward in the wild-type enzyme (Fig. 5B). These two loops (both located in the FAD binding domain [7]) display the same degree of flexibility in both wtFMO and FMOW47F (Fig. 5A, highlighted in pink). Thus, the difference in the loop movement might likely affect conformational changes important for catalysis (see below).

Table 3
Unfolding temperatures of wild-type and mutant FMO.

	wtFMO	FMOW47F
Alone	39.9 ± 0.1 °C	40.6 ± 0.1 °C
+$NADP^+$	41.9 ± 0.1 °C	40.8 ± 0.1 °C

Conditions: 30 μL 100 mM sodium phosphate, 5 μM enzyme, 25 μM SYPRO orange, and 100 μM $NADP^+$.

Protein stability

The MD results suggested that by replacing W at position 47 to F, some regions of the protein became more rigid. In order to determine the effect experimentally, we measured the melting temperature (T_m) of wtFMO and FMOW47F (Fig. 3S). In the absence of $NADP^+$, the mutant enzyme appeared to be more stable, but by only 0.7 °C (Table 3). Although, this is consistent with the MD results, the effect is very low. In the presence of $NADP^+$, the T_m value for wtFMO increased 2 °C. In contrast, the binding of $NADP^+$ did not result in an increase in the T_m value for the FMOW47F enzyme (Table 3). This is not due to a change in affinity for $NADP^+$ since the K_m value for this coenzyme was not affected by the mutation (Table 1). Instead, these results indicate that the mutant enzyme is more rigid, and this rigidity prevents it from acquiring the more stable enzyme-bound conformation observed for wtFMO. Thus, it is possible that conformational changes that are associated with the hydride transfer step are impaired in the mutant enzyme.

Conclusions

The active sites of flavin-dependent monooxygenases are fine-tuned to accommodate two substrates and oxygenated flavin intermediates during catalysis. As noted by Alfieri et al. [6], the position of $NADP^+$ observed in the structure is not optimal for hydride transfer (Fig. 1). Instead, this binding mode is essential for stabilization of the C4-hydroperoxyflavin (Scheme 1c). Thus, it was proposed that protein conformational changes must occur after or during hydride transfer [6]. These conformational changes are required to position $NADP^+$ in a conformation where it plays a role in stabilization of the C4a-hydroperoxyflavin–the position observed in the X-ray structure (Fig. 1B) [6,7,16]. The data presented here shows that mutation of W47, which is located on the *si*-face of the flavin ring, results in only a minimal effect in the oxidative half-reaction. This is consistent with results that indicate that oxygen activation and stabilization of C4a-hydroperoxyflavin occurs on the *re*-face of the flavin ring, where $NADP^+$ binds [7]. Replacement of W47 to F, results in a decrease in the rate of hydride transfer from NADPH to the flavin. MD simulations show that this mutation causes changes in the flexibility of the protein, including active site residues and the nicotinamide moiety of $NADP^+$. These minor changes translate into a more rigid FMOW47F protein. Thermal stability analysis shows that binding of $NADP^+$ causes the wild-type enzyme to become more thermally stable. This is consistent with the protein becoming more compact upon ligand binding. However, the FMOW47F enzyme does not become more thermally stable upon $NADP^+$ binding. We propose that due to the more rigid nature of the mutant enzyme, the conformational changes that occur during NADP(H) binding are prevented or minimized. These conformational changes might be necessary to properly align the NADP-C4 and FAD-N5 for hydride transfer. In fact, the simulations show that in wtFMO the NADP-C4 and FAD-N5 distance fluctuates more, perhaps allowing sampling of the optimal position for hydride transfer. In contrast, the NADP-C4 and FAD-N5 distance is less variable in the mutant protein, perhaps decreasing the rate of hydride transfer. Together, the data presented here

shows how the active site of flavin monooxygenases are exquisitely fine-tuned for catalysis, showing that even residues which are on the opposite side of the "active site" are important for modulating protein motions important for the chemical steps. Since this tryptophan residue is conserved in other members of the Class B flavin-monooxygenases, it is possible that it plays a similar role in the mechanism of action of other members of this family of enzymes.

Acknowledgments

This work was supported in part by a grant from the National Science Foundation MCB-1021384 and by a grant from the Virginia Academy of Sciences.

References

[1] W.J. van Berkel, N.M. Kamerbeek, M.W. Fraaije, J. Biotechnol. 124 (2006) 670–689.
[2] V. Massey, J. Biol. Chem. 269 (1994) 22459–22462.
[3] P. Chaiyen, M.W. Fraaije, A. Mattevi, Trends Biochem. Sci. 371 (2012) 373–380.
[4] N.B. Beaty, D.P. Ballou, J. Biol. Chem. 256 (1981) 4619–4625.
[5] D.M. Ziegler, Drug Metab. Rev. 34 (2002) 503–511.
[6] A. Alfieri, E. Malito, R. Orru, M.W. Fraaije, A. Mattevi, Proc. Natl. Acad. Sci. USA 105 (2008) 6572–6577.
[7] R. Orru, D.E. Pazmino, M.W. Fraaije, A. Mattevi, J. Biol. Chem. 285 (2010) 35021–35028.
[8] P.G. Blommel, P.A. Martin, K.D. Seder, R.L. Wrobel, B.G. Fox, Methods Mol. Biol. 498 (2009) 55–73.
[9] L.L. Poulsen, D.M. Ziegler, J. Biol. Chem. 254 (1979) 6449–6455.
[10] S.S. Jeong, J.E. Gready, Anal. Biochem. 221 (1994) 273–277.
[11] E. Romero, M. Fedkenheuer, S.W. Chocklett, J. Qi, M. Oppenheimer, P. Sobrado, Biochim. Biophys. Acta 1824 (2012) 850–857.
[12] C. Oostenbrink, A. Villa, A.E. Mark, W.F. Van Gunsteren, J. Comput. Chem. 25 (2004) 1656–1676.
[13] J.C. Gordon, J.B. Myers, T. Folta, V. Shoja, L.S. Heath, A. Onufriev, Nucleic Acids Res. 33 (2005) W368–W371.
[14] H.J.C. Berendsen, J.P.M. Postma, W.F. Van Gunsteren, J. Hermans, Intermolecular Forces, in: B. Pullman (Ed.), Reidel Dordrecht, The Netherlands, 1981, p. pp. 331.
[15] S. Badieyan, D.R. Bevan, C.M. Zhang, Protein Eng. Des. Sel. 25 (2012) 223–233.
[16] R. Orru, H.M. Dudek, C. Martinoli, D.E. Torres Pazmino, A. Royant, M. Weik, M.W. Fraaije, A. Mattevi, J. Biol. Chem. 286 (2011) 29284–29291.